 CMC, vol.29, no.2, pp.129-154, 2012

Domain-Decomposition Singular Boundary Method for Stress Analysis in Multi-Layered Elastic Materials

Yan Gu[1], Wen Chen[1,2] and Xiao-Qiao He[3]

Abstract: This paper applies an improved singular boundary method (SBM) in conjunction with domain decomposition technique to stress analysis of layered elastic materials. For problems under consideration, the interface continuity conditions are approximated in the same manner as the boundary conditions. The multi-layered coating system is decomposed into multiple subdomains in terms of each layer, in which the solution is approximated separately by the SBM representation. The singular boundary method is a recent meshless boundary collocation method, in which the origin intensity factor plays a key role for its accuracy and efficiency. This study also introduces new strong-form regularization formulas to accurately evaluate the origin intensity factors for elasticity problem. Consequently, we dramatically improve the accuracy and convergence of SBM solution of the elastostatics problems. The proposed domain-decomposition SBM is tested on two benchmark problems. Based on numerical results, we discuss merits of the present SBM scheme over the other boundary discretization methods, such as the method of fundamental solution (MFS) and the boundary element method (BEM).

Keywords: Multi-layered materials, singular boundary method, domain decomposition, meshless boundary collocation method, origin intensity factor, elasticity.

1 Introduction

In the machining industry, the coatings consist of one or more layers and protect the tool against adhesion diffusion and intensive abrasive wear and also provide a barrier for the intensive heat flow from the contact area into the substrate material. Thanks to their thin-walled structures, the boundary-only discertization techniques, typically boundary element method (BEM) [Atluri (2005); Cheng and

[1] College of Harbour, Coastal and Offshore Engineering, Hohai University, Nanjing 210098, PR China
[2] Corresponding author. E-mail: chenwen@hhu.edu.cn
[3] Department of Civil and Architectural Engineering, City University of Hong Kong, Hong Kong

Cheng (2005)], have the salient edges over domain discretization methods such as finite element method (FEM) in the numerical modeling of the problems of this type. However, the traditional BEM encounters challenging mesh generation for complex-shaped moving boundary problems and costly numerical integration.

To remedy the above-mentioned problems, recent decades have witnessed a quickly increasing research on the so-called meshless strong-form boundary collocation methods, among which the most known is the method of fundamental solution (MFS) [Chen et al. (1998); Fairweather and Karageorghis (1998); Golberg et al. (2000); Poullikkas et al. (2002)]. The MFS shares major advantages of the BEM over domain discretization methods [Cheng and Cheng (2005); Marin (2009)]. In addition, it has further advantages over the BEM in that it does not require an elaborate discretization of the boundary and avoids computationally expensive and mathematically tricky numerical integration. No extra quadratures are required to evaluate solutions in the interior domain as well. In addition, the MFS is mathematically simple and very easy to program with little data preparation. On the downside, the traditional MFS, however, requires a fictitious boundary for the placement of the source points to circumvent singularity of fundamental solution. The costly non-linear least-squares minimization procedure is sometimes used to determine this artificial boundary. In practice, the fictitious boundary is largely determined based on trial-error empirical law and can be arbitrary. This has long been a perplexing issue to restrict its utility in real-world problems.

The singular boundary method (SBM) [Chen et al. (2009); Chen and Wang (2010); Gu et al. (2011); Htike et al. (2011)] is another recent meshless boundary collocation method. Like the MFS, the SBM is an inherently meshless boundary collocation method [Chen et al. (2003); Liu et al. (2009); Sarler (2009); Wang et al. (2009); Young et al. (2005)] in which the mesh or element is not required and only boundary nodes are generated. The SBM enjoys all merits of the MFS and BEM. Its key idea is to introduce a concept of the origin intensity factor [Chen and Gu (2011); Gu et al. (2012a)] to isolate the singularity of the fundamental solutions in a strong-from integration-free fashion. Consequently, the solution of the problem of interest can be approximated by a linear combination of fundamental solutions with sources located directly on the physical boundary. This is dramatically different from the MFS in that the perplexing fictitious boundary is totally eliminated. Prior to this study, the SBM has been successfully used for the solution of many problems, such as potential problems [Chen and Wang (2010); Gu et al. (2012b)], infinite domain problems [Chen and Fu (2010)], and plane elasticity problems [Gu et al. (2011)].

As mentioned above, the origin intensity factor plays a key role in the SBM and its accurate evaluation can dramatically improve the accuracy, stability, and effi-

ciency of the SBM solution. This paper introduces new strong-form regularization formulas to accurately evaluate the origin intensity factors for elasticity problem. This study will apply this improved SBM scheme to stress analysis in multi-layered elastic materials. Different from our previous SBM solution of 2D elasticity problems [Gu et al. (2011)], our new regularization technique can accurately remove the singularities of the fundamental solution and its derivatives in the strong-form fashion, and consequently, the origin intensity factors can be determined directly without using any sample nodes as in Ref. [Gu et al. (2011)].

The multi-layered problems under consideration are solved using a domain decomposition technique (DDT), which has been successfully used in conjunction with the BEM and MFS, see Refs. [Berger and Karageorghis (1999); Berger and Karageorghis (2001); Chen and Liu (2001); Gao et al. (2007); Karageorghis and Lesnic (2008); Luo et al. (2000)]. The basic idea behind the DDT is that the whole domain of concern is broken up into separated subdomains and the final system of equations is constituted by assembling algebraic equations discretized in each subdomain, based on the compatibility of displacements and equilibrium of tractions at adjacent common interface nodes. The resulting algebraic equations have a blocked sparse coefficient matrix.

This paper is an extension of our recent work [Chen et al. (2011)] where a new regularization technique was derived and applied to 2D elastostatics problems. Herein, the developed SBM formulation is extended to multi-domain problems and applied to the stress analysis for multi-layered coating systems. A brief outline of the paper is as follows. In section 2, we introduce the SBM formulation in the solution of elastostatics problems in a single material. In section 3, we describe the SBM domain decomposition approach for the solution of multi-layered elastic problems. In section 4, two benchmark test problems are examined to validate the computational code and assess the performances of the proposed SBM scheme. Finally, the conclusions and remarks are provided in Section 5.

2 The SBM for elastostatics problem in a single material

In the absence of body forces, the equilibrium equations for plane elastostatics problem, also known as the Navier equations, with respect to the displacement components $u_i(x)$, $i = 1,2$, can be stated as

$$\left\{2\frac{1-\mu}{1-2\mu}\right\}\frac{\partial^2 u_1(x)}{\partial x_1^2}+\frac{\partial^2 u_1(x)}{\partial x_2^2}+\left\{\frac{1}{1-2\mu}\right\}\frac{\partial^2 u_2(x)}{\partial x_1 \partial x_2}=0,\ \ x\in\Omega \tag{1}$$

$$\left\{\frac{1}{1-2\mu}\right\}\frac{\partial^2 u_1(x)}{\partial x_1 \partial x_2}+\frac{\partial^2 u_2(x)}{\partial x_1^2}+\left\{2\frac{1-\mu}{1-2\mu}\right\}\frac{\partial^2 u_2(x)}{\partial x_2^2}=0,\ \ x\in\Omega \tag{2}$$

with the boundary conditions

$$u_i(x) = \bar{u}_i \quad x \in \Gamma_u \text{ (Dirichlet boundary conditions)}, \tag{3}$$

$$t_i(x) = \bar{t}_i \quad x \in \Gamma_t \text{ (Neumann boundary conditions)}, \tag{4}$$

where μ represents the Poisson's ratio, $t_i(x)$ denotes the component of boundary traction in the i^{th} coordinate direction, the boundary of Ω is $\partial\Omega = \Gamma_u \cup \Gamma_t$ which we assume to be piecewise smooth, $\bar{u}_i$ and $\bar{t}_i$ represent the prescribed displacements and tractions, respectively.

The strains $\varepsilon_{ij}(x),\ i,j = 1,2$, are related to the displacement gradients by the kinematic relations

$$\varepsilon_{ij}(x) = \frac{1}{2}\left\{\frac{\partial u_i(x)}{\partial x_j} + \frac{\partial u_j(x)}{\partial x_i}\right\}, \tag{5}$$

and the stresses $\sigma_{ij}(x),\ i,j,= 1,2$, are related to the strains via Hooke's law by

$$\sigma_{ij}(x) = 2G\left(\varepsilon_{ij}(x) + \frac{\mu}{1-2\mu}\varepsilon_{kk}(x)\delta_{ij}\right), \tag{6}$$

where G is the shear modulus and δ_{ij} the Kronecker delta symbol. We use the customary standard Cartesian notation for summation over repeated subscripts.

The boundary tractions $t_i(x)$, $i = 1,2$, are defined in terms of the stresses as

$$t_i(x) = \sigma_{ij}(x)n_j(x), \quad x \in \partial\Omega, \tag{7}$$

where $n_j(x)$ is the direction cosine of the unit outward normal vector at the boundary point x.

Employing indicial notation for the coordinates of points x and s, i.e. x_1, x_2 and s_1, s_2, respectively, the Kelvin fundamental solutions of the elastostatics governing equations (1) and (2) can be expressed as [Banerjee (1994)]

$$U_{ij}(x,s) = -\frac{1}{8\pi G(1-\mu)}\left\{(3-4\mu)\log r(x,s)\delta_{ij} - r_{,i}(x,s)r_{,j}(x,s)\right\},\ (i,j=1,2), \tag{8}$$

where $r(x,s)$ is the Euclidean distance between the collocation point x and source point s, $r_{,i}(x,s) = \frac{\partial r(x,s)}{\partial x_i} = \frac{x_i - s_i}{r(x,s)}$ expresses the partial derivative of the distance r with respect to x_i.

The fundamental solution of the tractions can be obtained by first calculating the fundamental solutions of strains and then applying Hooke's law and are stated as

$$\begin{aligned} T_{ij}(x,s) = &-\frac{1}{4\pi(1-\mu)r(x,s)}\left\{\left[(1-2\mu)\delta_{ij}+2r_{,i}(x,s)r_{,j}(x,s)\right]r_{,n}(x,s)\right. \\ &\left.+(1-2\mu)\left(r_{,i}(x,s)n_j(x)-r_{,j}(x,s)n_i(x)\right)\right\}, \quad (i,j=1,2), \end{aligned} \tag{9}$$

where $r_{,n}(x,s) = r_{,i}(x,s)n_i(x)$ represents the derivative of r in the direction of the outward normal at the point x. Similarly, the fundamental solution of stress is given by

$$\begin{aligned} D_{ijk}(x,s) = &\frac{1}{4\pi(1-\mu)r(x,s)}\left\{(1-2\mu)\left[r_{,k}(x,s)\delta_{ij}-r_{,j}(x,s)\delta_{ik}-r_{,i}(x,s)\delta_{jk}\right]\right. \\ &\left.-r_{,i}(x,s)r_{,j}(x,s)r_{,k}(x,s)\right\}, \quad (i,j,k=1,2). \end{aligned} \tag{10}$$

By analogy with the radial basis function (RBF) interpolation [Li et al. (2008); Marin and Lesnic (2004); Redekop and Cheung (1987); Saranen and Vainikko (2002)], the displacement and traction solutions can be approximated by a linear combination of fundamental solutions with respect to different sources s as follows:

$$u_i(x^m) = \sum_{n=1}^{N}\alpha_j(s^n)U_{ij}(x^m,s^n) = \sum_{n=1}^{N}\left\{\alpha_1(s^n)U_{i1}(x^m,s^n)+\alpha_2(s^n)U_{i2}(x^m,s^n)\right\}, \tag{11}$$

$$t_i(x^m) = \sum_{n=1}^{N}\alpha_j(s^n)T_{ij}(x^m,s^n) = \sum_{n=1}^{N}\left\{\alpha_1(s^n)T_{i1}(x^m,s^n)+\alpha_2(s^n)T_{i2}(x^m,s^n)\right\}, \tag{12}$$

where $i,j=1,2$, $x^m \in \Omega\cup\partial\Omega$ is the m^{th} collocation point and s^n the n^{th} source point, $\{\alpha_j(s^n)\}_{n=1}^N$ represent the n^{th} unknown coefficient of the distributed source at s^n, N denotes the numbers of source points.

In the traditional MFS, a fictitious boundary outside the problem domain is required in order to place the source points $\{s^n\}_{n=1}^N$ and avoid the singularity of the fundamental solutions. These source points are either pre-assigned or taken to be part of the unknowns of the problem along with the coefficients $\{\alpha_j(s^n)\}_{n=1}^N$. In the early applications of the MFS [Johnston and Fairweather (1984)], the locations of the source points were determined by a non-linear system of the equations that can be solved using a non-linear least-squares minimization software. This approach, however, has attracted limited attention primarily because of its high computational costs and the criticism that a linear boundary value problem is converted to a non-linear discrete problem [Karageorghis et al. (2011)]. In the recently established

fashion of the MFS the source points are pre-assigned, and the non-linear least-squares minimization procedure can be avoided. However, this introduces a perplexing problem of the optimal placement of the sources. In addition, the resulting global system matrix is badly conditioned, see for example [Chen et al. (2006)]. These drawbacks severely downplay the applicability of the MFS to real-world applications.

The SBM also uses the fundamental solution as the basis function of its approximation. However, unlike the MFS, the collocation and source points in the SBM are coincident and are both placed on the physical boundary without the need of using a fictitious boundary. The basic idea is to introduce a concept of the *origin intensity factor* to isolate the singularity of the fundamental solutions so that the source points can be placed on the real boundary directly. The SBM interpolation formulations for 2D elasticity problems can be expressed as [Gu et al. (2011)]

$$u_i(x^m) = \sum_{n=1,n\neq m}^{N} \alpha_j(s^n) U_{ij}(x^m,s^n) + \alpha_j(s^m) u_{ij}(x^m), \quad x^m \in \Gamma_u, \tag{13}$$

$$t_i(x^m) = \sum_{n=1,n\neq m}^{N} \alpha_j(s^n) T_{ij}(x^m,s^n) + \alpha_j(s^m) t_{ij}(x^m), \quad x^m \in \Gamma_t, \tag{14}$$

where $u_{ij}(x^m) = U_{ij}(x^m,x^m)$ and $t_{ij}(x^m) = T_{ij}(x^m,x^m)$ are defined as the origin intensity factors, i.e., the diagonal and sub-diagonal elements of the SBM interpolation matrix. The fundamental assumption of the SBM is the existence of origin intensity factors upon the singularity of the coincident source-collocation nodes for mathematically well-posed problems [Gu et al. (2012a)]. Our experiments show that origin intensity factors do exist and have a finite value depending merely on the distribution of discrete boundary nodes and their respective boundary conditions.

When the collocation point x^m approaches to the source point s^n, the distance between them tends to zero. Consequently, Eqs. (13) and (14) will present various orders of singularity. Therefore, these two formulations should be regularized by using some special treatments. By adopting a subtracting and adding-back technique [Anselone (1981); Chen and Gu (2011); Guiggiani (1991); Guiggiani and Gigante (1990)], the regularized SBM formulation for Neumann boundary condi-

tions (12) can be expressed as

$$\begin{aligned} t_i(x^m) &= \sum_{n=1}^{N} \alpha_j(s^n) T_{ij}(x^m, s^n) \\ &= \sum_{n=1}^{N} \left(\alpha_j(s^n) - \frac{L_n}{L_m} \alpha_j(x^m) \right) T_{ij}(x^m, s^n) \\ &+ \frac{\alpha_j(x^m)}{L_m} \sum_{n=1}^{N} \left[L_n T_{ij}(x^m, s^n) + L_n T_{ij}^{(\mathrm{E})}(s^n, x^m) \right], \end{aligned} \tag{15}$$

in which

$$\sum_{n=1}^{N} L_n T_{ij}^{(\mathrm{E})}(s^n, x^m) = 0, \quad i, j = 1, 2, \tag{16}$$

and $T_{ij}^{(\mathrm{E})}(s^n, x^m)$ denotes the fundamental solution of the exterior problems. The detailed derivations of Eq. (16) are provided in Appendix A. In the above equations (15) and (16), L_m represents the half distance between the source nodes s^{m-1} and s^{m+1}.

According to the dependency of the outward normal vectors on the two kernel functions of interior and exterior problems [Young et al. (2005)], we can obtain the following relationships

$$\begin{cases} T_{ij}(s^n, x^m) = -T_{ij}^{(\mathrm{E})}(s^n, x^m), & m \neq n, \\ T_{ij}(s^n, x^m) = T_{ij}^{(\mathrm{E})}(s^n, x^m), & m = n. \end{cases} \tag{17}$$

With the help of Eq. (17) and noting that $\alpha_j(s^n) - L_n \alpha_j(x^m)/L_m = 0$ when n is equal to m, the regularized Neumann boundary equation (15) can be rewritten as

$$\begin{aligned} t_i(x^m) &= \sum_{n=1, m \neq n}^{N} \left(\alpha_j(s^n) - \frac{L_n}{L_m} \alpha_j(x^m) \right) T_{ij}(x^m, s^n) \\ &+ \frac{\alpha_j(x^m)}{L_m} \left[L_m T_{ij}(x^m, s^m) + L_m T_{ij}(s^m, x^m) \right] \\ &+ \frac{\alpha_j(x^m)}{L_m} \sum_{n=1, m \neq n}^{N} \left[L_n T_{ij}(x^m, s^n) - L_n T_{ij}(s^n, x^m) \right]. \end{aligned} \tag{18}$$

Combining the similar terms produces

$$t_i(x^m) = \sum_{n=1,m\neq n}^{N} \alpha_j(s^n) T_{ij}(x^m,s^n) + \frac{\alpha_j(x^m)}{L_m} \Big\{ [L_m T_{ij}(x^m,s^m) + L_m T_{ij}(s^m,x^m)] - \sum_{n=1,m\neq n}^{N} L_n T_{ij}(s^n,x^m) \Big\}. \tag{19}$$

Since the collocation point x^m and the source point s^n will never coincide when m is unequal to n, both the terms $\sum_{n=1,m\neq n}^{N} \alpha_j(s^n) T_{ij}(x^m,s^n)$ and $\sum_{n=1,m\neq n}^{N} L_n T_{ij}(s^n,x^m)$ are regular and can directly be calculated without any special treatments. The remaining term $L_m T_{ij}(x^m,s^m) + L_m T_{ij}(s^m,x^m)$, however, will present singularity and is approximated by a quadrature rule as

$$\begin{aligned} I_m &= L_m T_{ij}(x^m,s^m) + L_m T_{ij}(s^m,x^m) \approx \int_{\Gamma_m} [T_{ij}(x^m,s) + T_{ij}(s,x^m)] d\Gamma_m(s) \\ &= \int_{\Gamma_m} \frac{k_1}{r} \left\{ r_{,l} \left[n_l(x^m) - n_l(s) \right] \left[k_2 \delta_{ij} + 2 r_{,i} r_{,j} \right] + k_2 r_{,i} \left[n_j(x^m) - n_j(s) \right] \right. \\ &\quad \left. - k_2 r_{,j} \left[n_i(x^m) - n_i(s) \right] \right\} d\Gamma_m(s), \end{aligned} \tag{20}$$

where $i,j,l = 1,2$, $k_1 = -1/4\pi(1-\mu)$, $k_2 = 1-2\mu$, $r = r(x^m,s)$, and $r_{,i} = r_{,i}(x^m,s)$. We can observe that when the collocation point x^m moves close to the source point s, the degree of the singularity of the integrand r is reduced or damped out by one order owing to the relative quantity $n_i(x^m) - n_i(s)$. Thus the whole integral is more amenable for numerical integration and can be accurately calculated by using the standard Gaussian quadrature. The integration domain is illustrated in Fig. 1.

Using the procedure described above, the final form of the regularized Neumann boundary equation can be expressed as

$$t_i(x^m) = \sum_{n=1,m\neq n}^{N} \alpha_j(s^n) T_{ij}(x^m,s^n) + \frac{\alpha_j(x^m)}{L_m} \left[I_m - \sum_{n=1,m\neq n}^{N} L_n T_{ij}(s^n,x^m) \right], \tag{21}$$

and then the aforementioned origin intensity factors can be extracted out as

$$t_{ij}(x^m) = \frac{1}{L_m} \left[I_m - \sum_{n=1,m\neq n}^{N} L_n T_{ij}(s^n,x^m) \right]. \tag{22}$$

After using the proposed regularized technique, we are able to remove or damp out the singularity of the kernel functions of the Neumann boundary equation. The

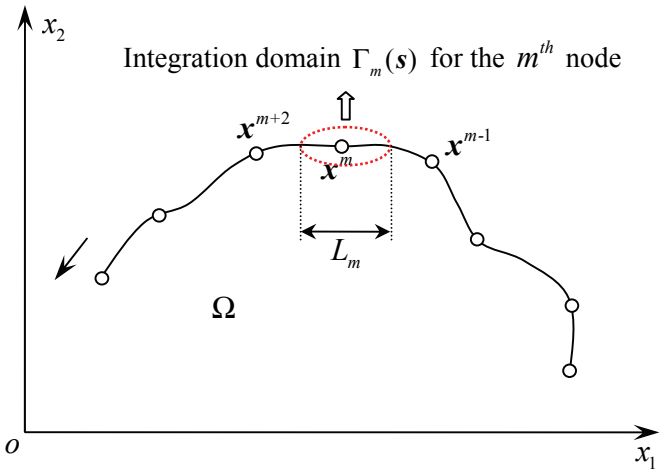

Figure 1: Nodal integration domain for 2D problem

matrix form of discretization equations (21) can be written as:

$$\begin{Bmatrix} t_1(x^1) \\ t_2(x^1) \\ \vdots \\ t_1(x^N) \\ t_2(x^N) \end{Bmatrix} = \begin{bmatrix} t_{11}(x^1) & t_{12}(x^1) & \cdots & T_{11}(x^1,s^N) & T_{12}(x^1,s^N) \\ t_{21}(x^1) & t_{22}(x^1) & \cdots & T_{21}(x^1,s^N) & T_{22}(x^1,s^N) \\ \vdots & \vdots & \ddots & \vdots & \vdots \\ T_{11}(x^N,s^1) & T_{12}(x^N,s^1) & \cdots & t_{11}(x^N) & t_{12}(x^N) \\ T_{21}(x^N,s^1) & T_{22}(x^N,s^1) & \cdots & t_{21}(x^N) & t_{22}(x^N) \end{bmatrix} \begin{Bmatrix} \alpha_1(s^1) \\ \alpha_2(s^1) \\ \vdots \\ \alpha_1(s^N) \\ \alpha_2(s^N) \end{Bmatrix} \tag{23}$$

On the other hand, the calculation of the origin intensity factors on Dirichlet boundary equations (11) can be directly set as an average value of the fundamental solution over a portion of the boundary. This can be formulated as

$$\begin{aligned} u_{ij}(x^m) &= \frac{1}{L_m}\int_{\Gamma_m(s)} U_{ij}(x^m,s)d\Gamma_m(s) \\ &= \frac{1}{L_m a_1}\int_{\Gamma_m(s)} a_2 \log r(x^m,s)\delta_{ij}d\Gamma_m(s) \\ &- \frac{1}{L_m a_1}\int_{\Gamma_m(s)} r_{,i}(x^m,s)r_{,j}(x^m,s)d\Gamma_m(s), \end{aligned} \tag{24}$$

where $a_1 = -8\pi G(1-\mu)$ and $a_2 = 3-4\mu$. Since there is no singularity in the second right hand side integral, it can be evaluated using a standard Gaussian quadra-

ture. The first right hand side integral, however, requires the following special treatment because of the weak singularity when the source point s moves closely to the collocation point x^m

$$\begin{aligned}\int_{\Gamma_m(s)} \log r(x^m,s)d\Gamma_m(s) &= \int_{-1}^{1} J(\xi)\log r(x^m,\xi)d\xi \\ &= \int_{-1}^{1} [J(\xi)-J(\eta)]\log r(x^m,\xi)d\xi \\ &+ J(\eta)\int_{-1}^{1} \log r(x^m,\xi)d\xi,\end{aligned} \tag{25}$$

where ξ is the intrinsic coordinate which transforms the integral so that it is mapped onto the interval [-1,1], $\eta \in [-1,1]$ denotes the position of the collocation point x^m, $J(\xi)$ represents the Jacobian of the transformation. These integrals can now be evaluated using the standard Gaussian quadrature and logarithmic schemes, respectively.

It is noteworthy that we calculate all SBM interpolation matrix elements directly in the strong-form fashion as in the MFS, except of the diagonal and sub-diagonal elements, namely original intensity factors, where the collocation points coincide with the source points. We only calculate these singular terms by using numerical integration and regularization schemes. This is dramatically different from various boundary element techniques where the numerical integration and mesh generation are required. Once all the boundary unknowns are solved, the displacements and stresses at any point inside the domain can be evaluated in a straight-forward fashion using Eqs. (13) and (14) which require no extra quadratures. Overall, this SBM scheme is unlike the weak-form BEMs and remains a strong form approach which greatly simplifies its implementations in programming and computational efficiency.

3 Domain-decomposition SBM for multi-layered materials

We considered a multi-layered elastic material coated with n layers (see Fig. 2). In such a case, all layers with each one being homogeneous, isotropic and linear elastic must be analyzed respectively. The boundary and interface conditions for each layer can be written as follows:

On the external surface of a coating layer, the traction must be given by

$$T_n = p_n, \;\; T_t = p_t, \tag{26}$$

where T_n and T_t are the normal and tangential components of the traction, p_n and p_t denote the loads applied in the normal and tangential direction, respectively

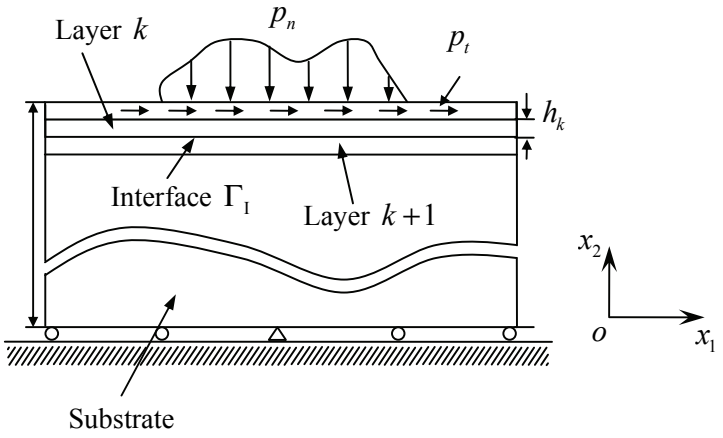

Figure 2: Notations for a multi-coated elastic solid

(see Fig. 2). In addition, the coating system should be constrained, with specified displacement, at some other locations on the boundary.

For a well-posed boundary value problem, there is only unknown (either displacements U or tractions T) at each nodal point on the boundary. However, along the interface Γ_I between layers k and $k+1$, both U and T are unknowns. To solve the problem numerically, there will be the same number of algebraic equations as the unknowns. Therefore, the following continuity conditions at the interface must be considered:

$$T_{In} = T_{In}^k = -T_{In}^{k+1}, \;\; T_{It} = T_{It}^k = -T_{It}^{k+1}, \tag{27}$$

$$U_{In} = U_{In}^k = U_{In}^{k+1}, \;\; U_{It} = U_{It}^k = U_{It}^{k+1}, \tag{28}$$

where the subscript In indicates interface I and normal (n) component, and subscript It represents interface I and tangential (t) direction.

First, the two layers k and $k+1$ with interface Γ_I, as shown in Fig. 2, are analyzed. In the k^{th} layer, the solution is approximated by the SBM-type expansion as

$$u_i^k(x^m) = \sum_{n=1, m\neq n}^{N} \alpha_j^k(s^n) U_{ij}^k(x^m, s^n) + \alpha_j^k(s^m) u_{ij}^k(x^m), \tag{29a}$$

$$t_i^k(x^m) = \sum_{n=1, m\neq n}^{N} \alpha_j^k(s^n) T_{ij}^k(x^m, s^n) + \alpha_j^k(s^m) t_{ij}^k(x^m), \tag{29b}$$

for $x^m \in \overline{\Omega^k}$, and, in the $(k+1)^{th}$ layer, the solution is approximated by

$$u_i^{k+1}(x^m) = \sum_{n=1,m\neq n}^{N} \alpha_j^{k+1}(s^n) U_{ij}^{k+1}(x^m, s^n) + \alpha_j^{k+1}(s^m) u_{ij}^{k+1}(x^m), \tag{30a}$$

$$t_i^{k+1}(x^m) = \sum_{n=1,m\neq n}^{N} \alpha_j^{k+1}(s^n) T_{ij}^{k+1}(x^m, s^n) + \alpha_j^{k+1}(s^m) t_{ij}^{k+1}(x^m), \tag{30b}$$

for $x^m \in \overline{\Omega^{k+1}}$, with an obvious extension of notation from Section 2.

The discretized algebraic equations from Eqs.(29) can be written in the matrix form as

$$\left[G^k\right]\left(\begin{Bmatrix}\alpha^k\end{Bmatrix}\right) = \left\{U^k\right\} \ , \ \left[G_I^k\right]\left(\begin{Bmatrix}\alpha^k\\ \alpha_I^k\end{Bmatrix}\right) = \left\{U_I^k\right\}, \tag{31a}$$

$$\left[H^k\right]\left(\begin{Bmatrix}\alpha^k\end{Bmatrix}\right) = \left\{T^k\right\} \ , \ \left[H_I^k\right]\left(\begin{Bmatrix}\alpha^k\\ \alpha_I^k\end{Bmatrix}\right) = \left\{T_I^k\right\}, \tag{31b}$$

where U_I^k, T_I^k and α_I^k are the interface displacements, tractions, and density functions of layer k on the interface Γ_I, U^k, T^k and α^k represent the displacements, tractions, and density functions of layer k on the remaining surfaces. G^k, G_I^k, H^k and H_I^k denotes the corresponding coefficient matrix containing the displacement or traction fundamental solutions.

Similarly, for the $(j+1)^{th}$ layer, we have the following equations

$$\left[G^{k+1}\right]\left(\begin{Bmatrix}\alpha^{k+1}\end{Bmatrix}\right) = \left\{U^{k+1}\right\} \ , \ \left[G_I^{k+1}\right]\left(\begin{Bmatrix}\alpha^{k+1}\\ \alpha_I^{k+1}\end{Bmatrix}\right) = \left\{U_I^{k+1}\right\}, \tag{32a}$$

$$\left[H^{k+1}\right]\left(\begin{Bmatrix}\alpha^{k+1}\end{Bmatrix}\right) = \left\{T^{k+1}\right\} \ , \ \left[H_I^{k+1}\right]\left(\begin{Bmatrix}\alpha^{k+1}\\ \alpha_I^{k+1}\end{Bmatrix}\right) = \left\{T_I^{k+1}\right\}. \tag{32b}$$

In order to illustrate the SBM procedures in a more clear fashion without loss of generality, we here suppose that the traction boundary conditions are prescribed on the external surfaces of k^{th} layer, and the displacement boundary conditions are prescribed on the external surfaces of $(k+1)^{th}$ layer. According to the equilibrium and compatibility conditions (27) and (28) at the interface, one has the following relations at the interface Γ_I

$$U_I^k = U_I^{k+1}, \ T_I^k = -T_I^{k+1}. \tag{33}$$

Hence, equations (31) and (32) can be coupled as

$$\begin{pmatrix} [H^k] & [0] \\ [G_I^k] & -[G_I^{k+1}] \\ [H_I^k] & [H_I^{k+1}] \\ [0] & [G^{k+1}] \end{pmatrix} \begin{bmatrix} \begin{pmatrix} \{\phi^k\} \\ \{\phi_I^k\} \end{pmatrix} \\ \begin{pmatrix} \{\phi^{k+1}\} \\ \{\phi_I^{k+1}\} \end{pmatrix} \end{bmatrix} = \begin{bmatrix} \{T^k\} \\ \{0\} \\ \{0\} \\ \{U^{k+1}\} \end{bmatrix}. \tag{34}$$

More equations can be added to this system in a similar way for other layers and the substrates. The system still needs to be reordered according to the prescribed displacement and traction boundary conditions. The system of equations (34) can be solved simultaneously for the boundary and interface unknowns. Once the boundary unknowns are solved, Eqs. (29) and (30) can be used to calculate the stress distributions at any point inside each subdomain.

4 Numerical examples and discussions

In order to assess the performance of the domain-decomposition SBM described in Sections 2 and 3, we solve in this section two benchmark numerical examples involving both smooth and piecewise smooth geometries. The effect of numerical accuracy, the convergence with respect to the number of boundary nodes, as well as the stability of the scheme with respect to the noise added into the input data are carefully investigated.

In real engineering applications, the known boundary data are often measured and thus inevitably contaminated by errors. Therefore, the stability of the numerical scheme is of vital importance to obtain physically meaningful results. To examine the stability of the SBM against contaminated data, the simulated noisy boundary data are generated in our test cases using the following formula:

$$\tilde{b} = b(1 + randn \times \delta), \tag{35}$$

where b is the exact data, *randn* is a normally distributed random variable with zero mean and unit standard deviation, and δ dictates the level of noise. In our computations, the random variable *randn* was realized using the Matlab function '*randn ()*'.

In order to measure the accuracy of the numerical approximation with respect to the exact solution, we use the relative error defined by

$$\text{Relative Error} = \left[\frac{1}{M} \sum_{k=1}^{M} \left(\frac{I^k_{\text{numerical}} - I^k_{exact}}{I^k_{exact}} \right)^2 \right]^{1/2}, \tag{36}$$

where $I^k_{\text{numerical}}$ and I^k_{exact} denote numerical and analytical solutions, respectively, at the k^{th} calculated point. Here, M is the total number of tested collocation points at which both the numerical and exact solutions are evaluated.

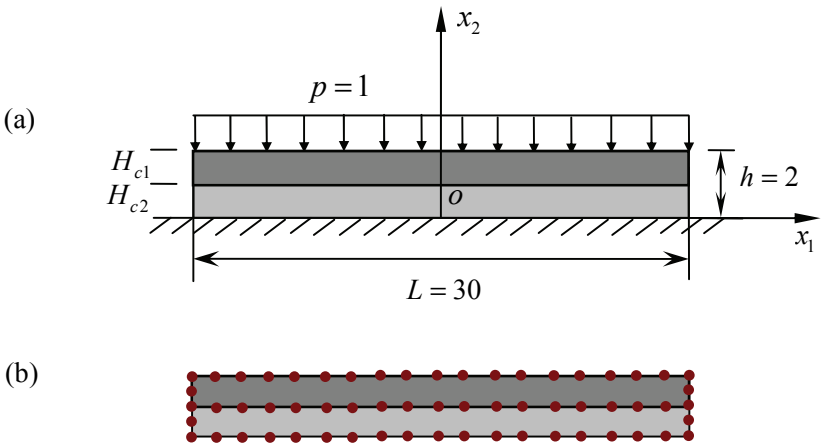

Figure 3: A two-layer coating system under constant pressure $p=1$ (Material constants are G=333333.333 Pa and $\mu=0.2$): (a) The geometry of the problem, and (b) the schematic distribution of source points using the SBM

4.1 Interfacial stress analysis for a two-layer coating system under uniform load

The first case is concerned with a symmetric two-layer coating system under a uniformly distributed load $p=1$ in the x_2-direction, where $H_{c1}=1$ is the thickness of the outside coating, $H_{c2}=1$ the thickness of the inside coating, $L=30$ the structure length. The geometric configuration of the problem and the distribution of the sources are schematically shown in Fig. 3. We assume the length of the plate in the x_3-direction is so large that this problem can be simplified to a plane strain problem. Because the dimension of the length $L=30$ is large compared to the dimension of the coatings ($h=H_{c1}+H_{c2}=2$), analytical solution of the whole system may be well approximated by considering the whole system as an elastic half-space. The bottom edge of the model is fixed, and thus, displacement components along the boundary $x_2=0$ in both the x_1- and x_2- directions are constrained. When the materials of the two coatings are identical, the analytical solution can be found readily

[Johnson (1985)] as

$$\begin{cases} \sigma_{11} = -\frac{\mu}{1-\mu},\ \sigma_{22} = -1,\ \sigma_{12} = 0 \\ u_1 = 0,\ u_2 = -\frac{1-2\mu}{2G(1-\mu)} x_2 \end{cases} \tag{37}$$

It is assumed that both coatings are composed of the identical material and share the same elastic constants. The analytical stress/displacement solutions of this case exist and can be obtained. In this special case, the stress distributions are in fact the internal stress components in the single material. The SBM domain decomposition approach is applied here simply to obtain these stresses inside this single material domain, in order to compare with the analytical solution.

In the SBM model, the horizontal boundaries are divided each into 80 boundary nodes, whereas the vertical ones into 20 boundary nodes each. Note that only 280 nodes are required in modeling the whole system since the nodes over the interfaces are shared by both coatings. We also provide the numerical results by the MFS and the BEM for the purpose of a fair comparison. It is noted that the BEM results are obtained using the direct formulation developed in Ref. [Banerjee (1994)]. For the MFS results, the sources are located on pseudo-boundaries which enclose the original domain and appear like physical boundary with a distance $d > 0$ in between. On each pseudo-boundary of the MFS, the sources are distributed in a similar way corresponding to the collocation nodes on the physical boundary. The schematic distribution of the fictitious source and boundary collocation points of the MFS is illustrated in Fig. 4.

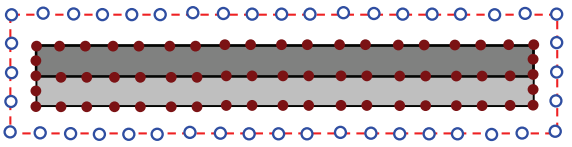

Figure 4: The distribution of the source (○) and boundary collocation (●) points in the MFS

Figs. 5 and 6 display the relative error curves of normal stresses σ_{11} and σ_{22} at interior points on the coating-coating interface ($x_2 = 1$) for varied values of x_1. As shown in these figures, the results of the present SBM are in very good agreement with the available analytical solutions, with the largest relative error less than 0.01, indicating its high accuracy and stability. We can also observe that the SBM results are slightly better than those of the BEM, possibly because the SBM requires no extra quadratures to evaluate solutions in the interior of the domain. Further, we

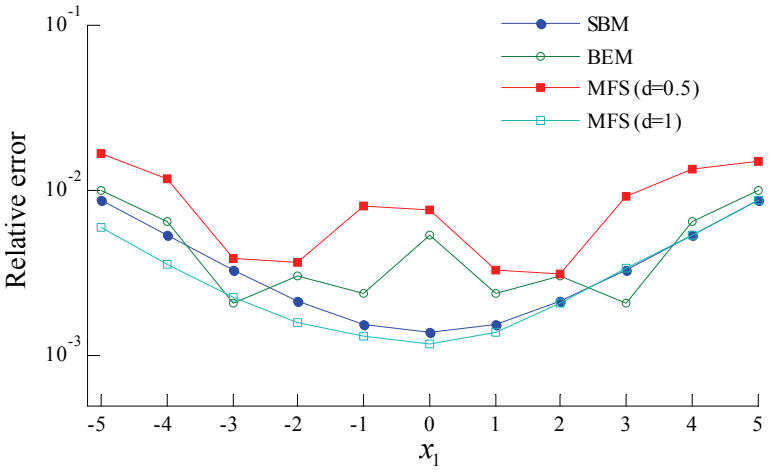

Figure 5: Relative error curves of normal stress σ_{11} at interior points on the coating-coating interface for varying values of x_1

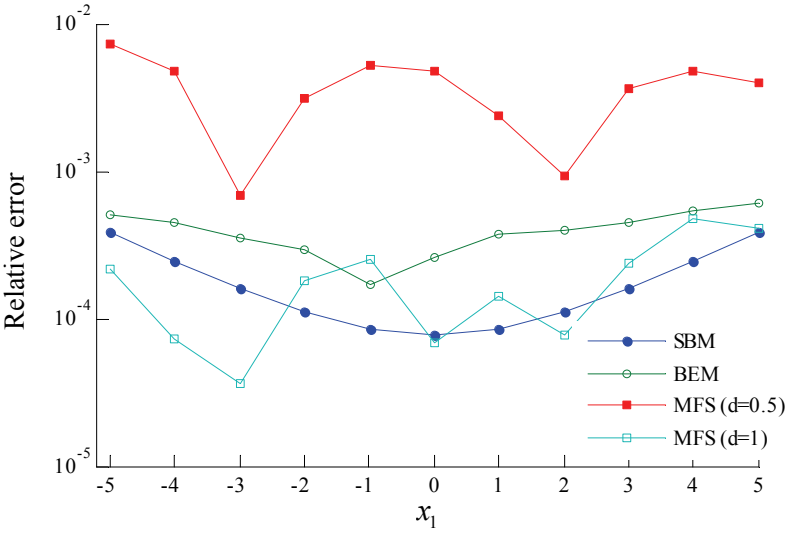

Figure 6: Relative error curves of normal stress σ_{22} at interior points on the coating-coating interface for varying values of x_1

can observe that the MFS solution accuracy with the fictitious boundary $d = 0.5$ dramatically deteriorates compared with $d = 1$, where d is an indicator of the fictitious boundary location, namely, the distance between the fictitious and the real boundaries. This clearly illustrates the decisive role of the fictitious boundary in the MFS performances. Although an appropriate or optimal placement of the fictitious boundary in the MFS can result in a very accurate solution, it remains an open issue to find this appropriate fictitious boundary for the real-word complex-shaped boundary problems.

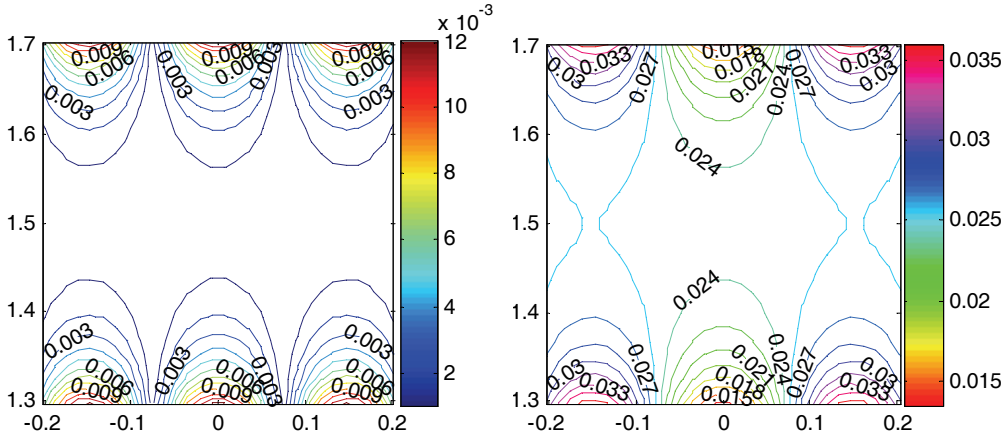

Figure 7: The domain-decomposition SBM error distribution of the normal stress σ_{11} calculated using exact (a) and 5% noise added into input data (b)

To investigate the stability, Figs. 7(a) and (b) present the error distribution of the normal stress σ_{11}, calculated via exact and 5% noise added into the input data, respectively, where the error curves were yielded at 30×30 calculation points uniformly-spaced over the square $(-0.2, 0.2) \times (1.3, 1.7)$. As shown in Fig. 7(a), the proposed SBM scheme is extremely accurate for problems with exact data, e.g. the maximum relative error 12×10^{-3}. It can be seen from Fig. 7(b) that the SBM results are in very good agreement with the analytical solutions even for a relatively high amount ($\delta = 5\%$) of noise added into the input data, reflecting the high stability. Similar results have also been obtained for the normal stress σ_{22}, as illustrated in Fig. 8. Hence we can conclude that the SBM in conjunction with the domain decomposition technique can provide stable and accurate numerical solutions to multi-layered elastic problems.

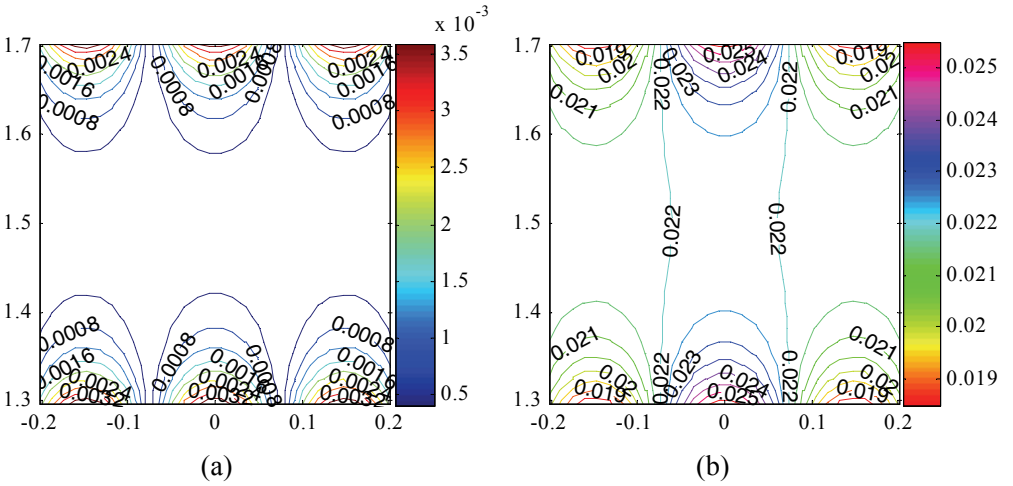

Figure 8: The domain-decomposition SBM error distribution of the normal stress σ_{22} calculated using exact (a) and 5% noise added into input data (b)

4.2 A rigid cylinder with two-layers of coatings

This test is concerned with a rigid shaft with two-layers of coatings under uniform pressure p, as shown in Fig. 9 where the layers of coatings consist of different materials (Young's modulus of outside coating/Young's modulus of inner coating=1/2 and Poisson ratio of outside coating=Poisson ratio of inner coating=0.2). The shaft and the two coatings have outer radii $r_1 = 5$, $r_2 = 6$ and $r_3 = 7$, respectively. It is assumed that the coatings are free to expand laterally except at the interface to the rigid shaft, but are axially constrained so that a condition of plane strain exists relative to $x_1 - x_2$ plane. This coating system is loaded by a uniform pressure $p = 1$, distributed around the circumference of the outside coating.

The boundary conditions of the displacement, under the rigid shaft assumption, are $u_r = u_\theta = 0$ for all nodes at the shaft-coating interface. Under such boundary conditions, the analytical solutions corresponding to this coating system is given by

$$\sigma_r = \frac{-13.2173}{r^2} - 0.7302, \ \sigma_\theta = \frac{13.2173}{r^2} - 0.7302, \tag{38}$$

for the outside coating and

$$\sigma_r = \frac{-11.6196}{r^2} - 0.7746, \ \sigma_\theta = \frac{11.6196}{r^2} - 0.7746, \tag{39}$$

for the inner coating, respectively, where (r,θ) denotes the polar coordinates.

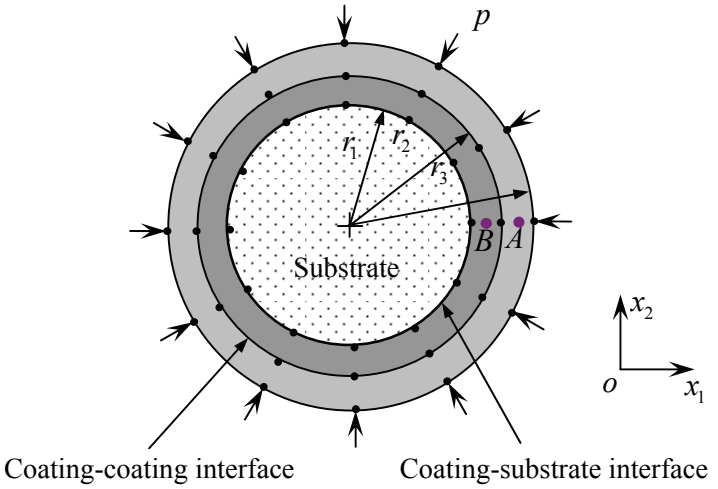

Figure 9: Cross-section of a shaft with two-layers of coatings

To investigate the convergence rate of relative error versus the number of boundary nodes, the convergence curves of the radial (σ_r) and tangential (σ_θ) stresses at interior points A and B are illustrated in Fig. 10, plotted in the log-log scale. It can be seen from this figure that when the number of boundary nodes increases, the relative errors decrease until the number of boundary nodes reaches $N = 360$, and thereafter more boundary nodes does not substantially improve the accuracy of the numerical results. This shows that accurate numerical results can be obtained using even relatively a small number of source points. Approximately, a convergence rate of 3.65, i.e., $O\left((1/N)^{3.65}\right)$, is estimated with respect to the number of boundary nodes, as shown by the dash-dot line in Fig. 10. Therefore, it could be concluded that, in general, the numerical solutions show a super convergence as the number of boundary nodes increases.

Next, we examine the SBM sensitivity of the numerical results with respect to the level of noise added into the input data. The SBM results for σ_r and σ_θ at interior points on the line $x_2 = 0$, computed using exact, 1% and 5% noise added into input data, are illustrated in Figs. 11 and 12, respectively. We can observe from these figures that even in the case of a relatively high amount ($\delta = 5\%$) of noise added into the input data, the proposed method produces good approximations in compar-

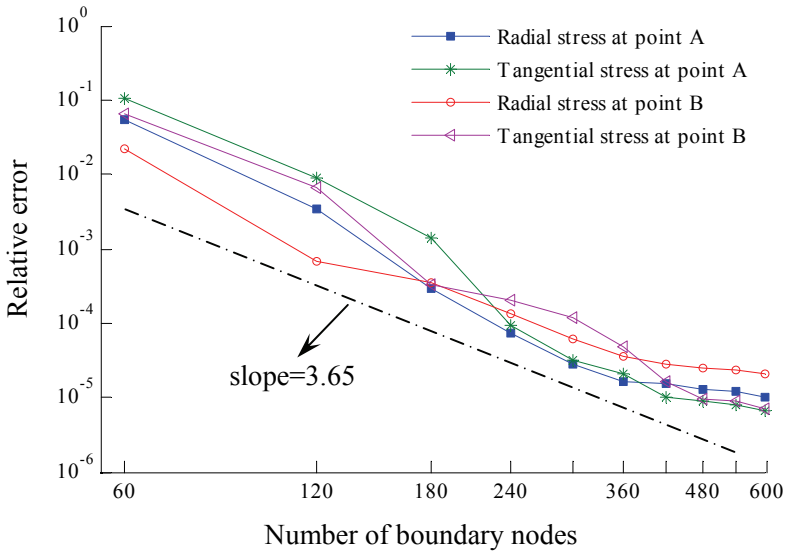

Figure 10: Convergence curves of the radial (σ_r) and tangential (σ_θ) stresses at interior points A and B

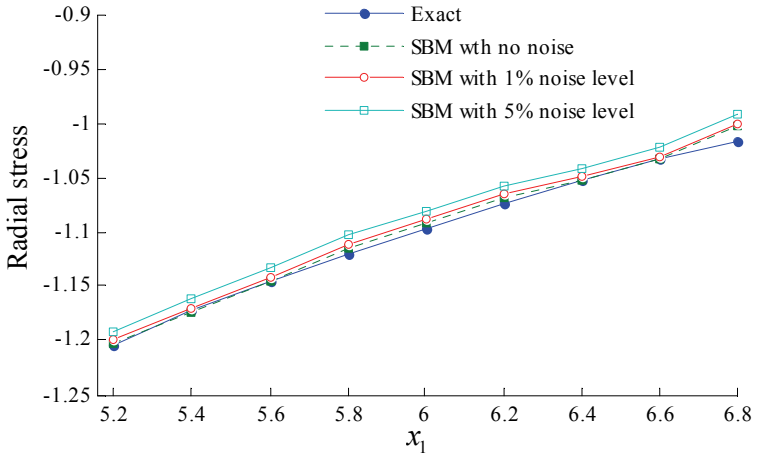

Figure 11: The analytical radial stress solution and domain-decompostion SBM results via exact and various amount of noise added into input data

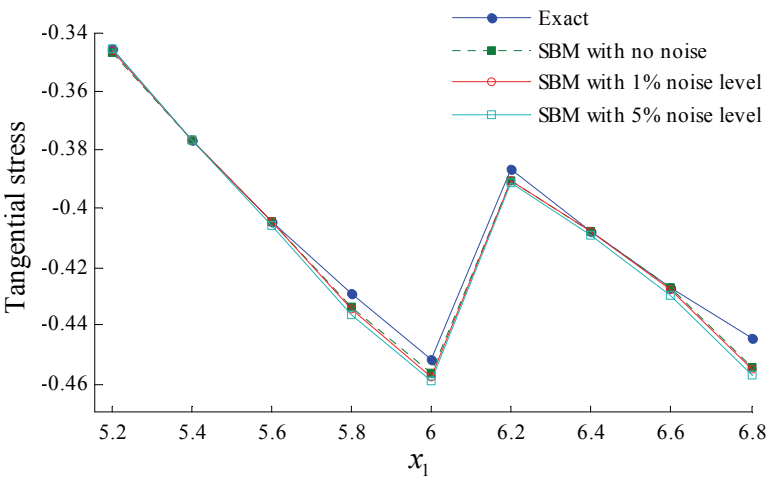

Figure 12: The analytical tangential stress solution and domain-decompostion SBM results via exact and various amount of noise added into input data

ison with analytical values. Furthermore, it should be mentioned that, as expected, the numerical stresses converge towards their corresponding exact solutions as the amount of noise decreases. Although not presented for the sake of limited space, it should be mentioned that we have performed numerous numerical experiments on the other cases and similar observations have been drawn.

5 Conclusions

In this paper, we developed a novel SBM domain decomposition technique to solve multi-layered elastic problems. The SBM is similar to the MFS in that both methods are meshless boundary collocation method with boundary-only nodes and no meshes requirement. The SBM, however, overcomes the fictitious boundary perplexing the MFS, thanks to the introduction of the concept of the origin intensity factor to isolate the singularity of the fundamental solutions. Compared with the BEM, the SBM is meshless easy to implement, and requires little data preparation, and avoids potentially troublesome extra quadratures to evaluate solutions in the interior of the domain. Thus, the SBM avoids the major drawbacks of meshless boundary methods and boundary element method, while keeping all their merits.

In the present domain-decompostion SBM scheme, the multi-layered problems under consideration are decomposed into several subdomains, and in each subdomain,

the solution is approximated by the SBM-type expansion. On the subdomain interfaces, the continuity of the displacements and the tractions is imposed. In addition, we also introduce new accurate formulas to calculate the origin intensity factors which play an important role in the SBM. From the foregoing numerical results, it can be concluded that the proposed scheme is computationally efficient, robust, accurate, stable with respect to decreasing noise added into the input data, and convergent with respect to increasing number of boundary nodes. In comparison with the other existing numerical methods for layered elastic problems, the proposed scheme could be considered as a competitive alternative.

Acknowledgement: The work described in this paper was supported by the National Basic Research Program of China (973 Project No. 2010CB832702), the National Science Funds for Distinguished Young Scholars of China (11125208), the R&D Special Fund for Public Welfare Industry (Hydrodynamics, Project No. 201101014), the research grant from the Research Grants Council of the Hong Kong Special Administrative Region (No. CityU 113809), and Jiangsu Province Graduate Students Research and Innovation Plan (No. CXZZ11_0424).

References

Anselone, P.M. (1981): Singularity subtraction in the numerical solution of integral equations. *J. Austral. Math. Soc. (Series B)*, vol. 22, no. 04, pp. 408-418.

Atluri, S.N. (2005): *Methods of computer modeling in engineering and the sciences*. Tech. Science Press.

Banerjee, P.K. (1994): *The boundary element methods in engineering*. McGRAW-HILL Book Company Europe.

Berger, J.R.; Karageorghis, A. (1999): The method of fundamental solutions for heat conduction in layered materials. *International Journal for Numerical Methods in Engineering*, vol. 45, no. 11, pp. 1681-1694.

Berger, J.R.; Karageorghis, A. (2001): The method of fundamental solutions for layered elastic materials. *Engineering Analysis with Boundary Elements*, vol. 25, no. 10, pp. 877-886.

Chen, C.S.; Cho, H.A.; Golberg, M.A. (2006): Some comments on the ill-conditioning of the method of fundamental solutions. *Engineering Analysis with Boundary Elements*, vol. 30, no. 5, pp. 405-410.

Chen, C.S.; Golberg, M.A.; Hon, Y.C. (1998): The method of fundamental solutions and quasi-Monte-Carlo method for diffusion equations. *International Journal for Numerical Methods in Engineering*, vol. 43, no. 8, pp. 1421-1435.

Chen, J.T.; Chen, W.C.; Lin, S.R.; Chen, I.L. (2003): Rigid body mode and spurious mode in the dual boundary element formulation for the Laplace problems. *Computers & Structures*, vol. 81, no. 13, pp. 1395-1404.

Chen, W.; Fu, Z. (2010): A novel numerical method for infinite domain potential problems. *Chinese Science Bulletin*, vol. 55, no. 16, pp. 1598-1603.

Chen, W.; Fu, Z.J.; Wei, X. (2009): Potential problems by singular boundary method satisfying moment condition. *CMES: Computer Modeling in Engineering & Sciences*, vol. 54, no. 1, pp. 65-85.

Chen, W.; Gu, Y. (2011): Recent advances on singular boundary method. *Joint International Workshop on Trefftz Method VI and Method of Fundamental Solution II, Taiwan*, no., pp.

Chen, W.; Gu, Y.; He, X. (2011): Improved singular boundary method for elasticity problems. *Journal of engineering mechanics*, vol. submitted, no., pp.

Chen, W.; Wang, F.Z. (2010): A method of fundamental solutions without fictitious boundary. *Engineering Analysis with Boundary Elements*, vol. 34, no. 5, pp. 530-532.

Chen, X.L.; Liu, Y.J. (2001): Thermal stress analysis of multi-layer thin films and coatings by an advanced boundary element method. *CMES:Computer Modeling in Engineering & Sciences*, vol. 2, no. 3, pp. 337-349.

Cheng, A.H.D.; Cheng, D.T. (2005): Heritage and early history of the boundary element method. *Engineering Analysis with Boundary Elements*, vol. 29, no. 3, pp. 268-302.

Fairweather, G.; Karageorghis, A. (1998): The method of fundamental solutions for elliptic boundary value problems. *Advances in Computational Mathematics*, vol. 9, no. 1, pp. 69-95.

Gao, X.W.; Guo, L.; Zhang, C. (2007): Three-step multi-domain BEM solver for nonhomogeneous material problems. *Engineering Analysis with Boundary Elements*, vol. 31, no. 12, pp. 965-973.

Golberg, M.A.; Chen, C.S.; Ganesh, M. (2000): Particular solutions of 3D Helmholtz-type equations using compactly supported radial basis functions. *Engineering Analysis with Boundary Elements*, vol. 24, no. 7-8, pp. 539-547.

Gu, Y.; Chen, W.; Zhang, C.Z. (2011): Singular boundary method for solving plane strain elastostatic problems. *International Journal of Solids and Structures*, vol. 48, no. 18, pp. 2549-2556.

Gu, Y.; Chen, W.; Zhang, J. (2012a): Investigation on near-boundary solutions by singular boundary method. *Engineering Analysis with Boundary Elements*, vol. 36, no. 8, pp. 1173-1182.

Gu, Y.; Chen, W.; He, X.-Q. (2012): Singular boundary method for steady-state heat conduction in three dimensional general anisotropic media. *International Journal of Heat and Mass Transfer*, vol. 55, no. 17-18, pp. 4837-4848.

Guiggiani, M. (1991): The evaluation of cauchy principal value integrals in the boundary element method—a review. *Mathematical and Computer Modelling*, vol. 15, no. 3–5, pp. 175-184.

Guiggiani, M.; Gigante, A. (1990): A General Algorithm for Multidimensional Cauchy Principal Value Integrals in the Boundary Element Method. *Journal of Applied Mechanics*, vol. 57, no. 4, pp. 906-915.

Htike, H.; Chen, W.; Gu, Y. (2011): Singular Boundary Method for Heat Conduction in Layered Materials. *CMC: Computers Materials & Continua*, vol. 24, no. 1, pp. 1-14.

Johnson, K.L. (1985): *Contact mechanics*. Cambridge University Press.

Johnston, R.L.; Fairweather, G. (1984): The method of fundamental solutions for problems in potential flow. *Applied Mathematical Modelling*, vol. 8, no. 4, pp. 265-270.

Karageorghis, A.; Lesnic, D. (2008): Steady-state nonlinear heat conduction in composite materials using the method of fundamental solutions. *Computer Methods in Applied Mechanics and Engineering*, vol. 197, no. 33-40, pp. 3122-3137.

Karageorghis, A.; Lesnic, D.; Marin, L. (2011): A survey of applications of the MFS to inverse problems. *Inverse Problems in Science and Engineering*, vol. 19, no. 3, pp. 309 - 336.

Li, Z.C.; Lu, T.T.; Hu, H.Y.; Cheng, A. (2008): *Trefftz and collocation methods*. WIT Press.

Liu, G.R.; Nguyen-Thoi, T.; Nguyen-Xuan, H.; Lam, K.Y. (2009): A node-based smoothed finite element method (NS-FEM) for upper bound solutions to solid mechanics problems. *Computers & Structures*, vol. 87, no. 1–2, pp. 14-26.

Luo, J.F.; Liu, Y.J.; Berger, E.J. (2000): Interfacial stress analysis for multi-coating systems using an advanced boundary element method. *Computational Mechanics*, vol. 24, no. 6, pp. 448-455.

Marin, L. (2009): An alternating iterative MFS algorithm for the Cauchy problem in two-dimensional anisotropic heat conduction. *CMC: Computers, Materials & Continua*, vol. 12, no. 1, pp. 71-100.

Marin, L.; Lesnic, D. (2004): The method of fundamental solutions for the Cauchy problem in two-dimensional linear elasticity. *International Journal of Solids and Structures*, vol. 41, no. 13, pp. 3425-3438.

Poullikkas, A.; Karageorghis, A.; Georgiou, G. (2002): The method of funda-

mental solutions for three-dimensional elastostatics problems. *Computers & Structures*, vol. 80, no. 3-4, pp. 365-370.

Redekop, D.; Cheung, R.S.W. (1987): Fundamental solutions for the collocation method in three-dimensional elastostatics. *Computers & Structures*, vol. 26, no. 4, pp. 703-707.

Saranen, J.; Vainikko, G. (2002): *Periodic integral and pseudodifferential equations with numerical approximation*. Springer Verlag.

Sarler, B. (2009): Solution of potential flow problems by the modified method of fundamental solutions: Formulations with the single layer and the double layer fundamental solutions. *Engineering Analysis with Boundary Elements*, vol. 33, no. 12, pp. 1374-1382.

Wang, F.Z.; Ling, L.; Chen, W. (2009): Effective condition number for boundary knot method. *CMC: Computers, Materials, & Continua*, vol. 12, no. 1, pp. 57-70.

Young, D.L.; Chen, K.H.; Lee, C.W. (2005): Novel meshless method for solving the potential problems with arbitrary domain. *Journal of Computational Physics*, vol. 209, no. 1, pp. 290-321.

Appendix A The detailed derivations of Eq. (16)

The null-field of the boundary integral equation (BIE) based on the direct method is given by

$$0=\int_{\Gamma}\left[U_{ij}^{(\mathrm{E})}(s,x^m)t_i(s)-T_{ij}^{(\mathrm{E})}(s,x^m)u_i(s)\right]d\Gamma(s),\quad x^m\in\Omega^{(\mathrm{E})},\tag{A1}$$

where $i,j=1,2$, the superscript (E) denotes the exterior domain, s is the source point located on the physical boundary and x^m is the field point.

Substituting the particular solution ($t_1(s)=t_2(s)=0$ when $u_1(s)=1$ and $u_2(s)=0$) into the above equation, we have

$$\int_{\Gamma}T_{11}^{(\mathrm{E})}(s,x^m)d\Gamma(s)=\int_{\Gamma}T_{12}^{(\mathrm{E})}(s,x^m)d\Gamma(s)=0,\quad x^m\in\Omega^{(\mathrm{E})}.\tag{A2}$$

In a similar way, substituting the particular solution ($t_1(s)=t_2(s)=0$ when $u_1(s)=0$ and $u_2(s)=1$) into the above equation A.1, we have

$$\int_{\Gamma}T_{21}^{(\mathrm{E})}(s,x^m)d\Gamma(s)=\int_{\Gamma}T_{22}^{(\mathrm{E})}(s,x^m)d\Gamma(s)=0,\quad x^m\in\Omega^{(\mathrm{E})}.\tag{A3}$$

We can rewrite Eqs. (A.2) and (A.3) as

$$\int_{\Gamma}T_{ij}^{(\mathrm{E})}(s,x^m)d\Gamma(s)=0,\quad i,j=1,2,\quad x^m\in\Omega^{(\mathrm{E})}.\tag{A4}$$

When the field point x^m approaches the boundary, we can discretize the Eq. (A.4) by

$$\int_\Gamma T_{ij}^{(\mathrm{E})}(s,x^m)d\Gamma(s) = \sum_{n=1}^{N}\int_{\Gamma_n} T_{ij}^{(\mathrm{E})}(s,x^m)d\Gamma_n(s) \approx \sum_{n=1}^{N} T_{ij}^{(\mathrm{E})}(s^n,x^m)L_n = 0$$
$$i,j=1,2, \quad x^m \in \Gamma. \quad \text{(A5)}$$

where L_n represents the half of distance of the $(n-1)^{th}$ and $(n+1)^{th}$ source points. Thus, we have

$$\sum_{n=1}^{N} L_n T_{ij}^{(\mathrm{E})}(s^n,x^m) = 0 \quad i,j=1,2, \quad x^m \in \Gamma, \quad \text{(A6)}$$

which is Eq. (16) in Section 2.